Finite element-based reliability assessment of quay walls

Roubos, A. A.; Schweckendiek, T.; Brinkgreve, R. B. J.; Steenbergen, R. D. J. M.; Jonkman, S. N.

DOI
10.1080/17499518.2020.1756344

Publication date
2020

Document Version
Final published version

Published in
Georisk: assessment and management of risk for engineered systems and geohazards

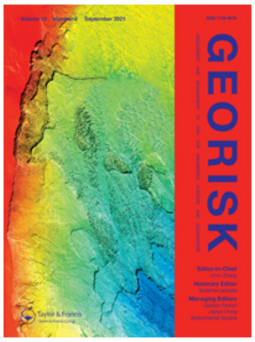

Taylor & Francis
Taylor & Francis Group

Georisk: Assessment and Management of Risk for Engineered Systems and Geohazards

ISSN: (Print) (Online) Journal homepage: https://www.tandfonline.com/loi/ngrk20

Finite element-based reliability assessment of quay walls

A. A. Roubos, T. Schweckendiek, R. B. J. Brinkgreve, R. D. J. M. Steenbergen & S. N. Jonkman

To cite this article: A. A. Roubos, T. Schweckendiek, R. B. J. Brinkgreve, R. D. J. M. Steenbergen & S. N. Jonkman (2021) Finite element-based reliability assessment of quay walls, Georisk: Assessment and Management of Risk for Engineered Systems and Geohazards, 15:3, 165-181, DOI: 10.1080/17499518.2020.1756344

To link to this article: https://doi.org/10.1080/17499518.2020.1756344

GEORISK
2021, VOL. 15, NO. 3, 165–181
https://doi.org/10.1080/17499518.2020.1756344

Finite element-based reliability assessment of quay walls

A. A. Roubos[a], T. Schweckendiek[a], R. B. J. Brinkgreve[a], R. D. J. M. Steenbergen[b] and S. N. Jonkman[a]

[a]Department of Hydraulic Engineering, Delft University of Technology, Delft, Netherlands; [b]Department of Structural Engineering, Ghent University, Ghent, Belgium

ABSTRACT

While reliability methods have already been widely adopted in civil engineering, the efficiency and robustness of finite element-based reliability assessments of quay walls are still fairly low. In this paper, the reliability indices of structural and geotechnical failure modes of two real-life quay walls are determined by coupling probabilistic methods with finite element models, taking into account a large number of stochastic variables. The reliability indices found are within the range of the targets suggested in the design codes presently in use. Nevertheless, neglecting model uncertainty and correlations between stochastic variables leads to an underestimation of the probability of failure. In addition, low sensitivity factors are found for time-independent variables, such as material properties and model uncertainty. Furthermore, the results are used to reflect on the partial factors used in the original design. Important variables, such as the angle of internal friction, are subjected to a sensitivity analysis in order to illuminate their influence on the reliability index. Port authorities and terminal operators might be able to use the findings of this paper to derive more insight into the reliability of their structures and to optimise their service life and functionality, for example by deepening berths or increasing operational loads.

ARTICLE HISTORY
Received 17 May 2019
Accepted 16 January 2020

KEYWORDS
Quay wall; reliability; finite elements; partial factors

1. Introduction

Quay walls are marine structures that ensure safe and efficient handling of ships. Since they frequently have a complex soil-structure interaction (e.g. due to inclined retaining walls or relieving platforms), structural and geotechnical assessments are usually performed semi-probabilistically while modelling the quay wall on the basis of finite elements. A more systematic way to account for uncertainties is to perform a reliability-based assessment (Phoon and Retief 2016). However, the efficiency and robustness of finite element-based reliability assessments in quay-wall engineering are rather low. In particular, it is still quite a challenge to achieve a robust coupling between probabilistic methods and finite element models, e.g. due to the highly complex and non-linear character of soil behaviour. Although a few studies (Rippi and Texeira 2016; Schweckendiek et al. 2012; Teixeira et al. 2016; Wolters, Bakker, and Gijt 2012) show promising results for quay walls and other soil-retaining structures, most use simplified models, distinguish a limited number of stochastic variables and they generally do not consider real-life structures.

The aim of this paper is to perform finite element-based reliability assessments of real-life quay walls taking into account a realistic number of stochastic variables in order to determine which design aspects are relevant to consider, to obtain insight into the reliability level of a quay wall designed in accordance with the Eurocode and to evaluate the partial factors of safety applied in the original design. As part of this study, a new reliability interface named ProbAna® (Laera and Brinkgreve 2017) was developed to couple Plaxis – an advanced finite element software package presently used in quay-wall engineering and geotechnical engineering in general – with the open source probabilistic toolbox OpenTURNS ("Open source initiative for the treatment of uncertainties, risks and statistics"). The outcomes were evaluated by performing reliability-based assessments using alternative reliability tools and design methods. The novelty of this study is that the reliability of two real-life quay walls having a fairly complex soil-structure interaction was estimated, while taking into account a large number of random variables. The two reference quay walls have been built in the port of Rotterdam and their designs comply with the Eurocode standard (NEN 1997, 2004). Furthermore, both structures are equipped with sensors, which were used to verify the quality of the finite element model.

2. Method for finite element-based reliability assessment of quay walls

2.1. Introduction

This section briefly introduces the information and methods used to perform finite element-based reliability

CONTACT A. A. Roubos aa.roubos@portofrotterdam.com, a.a.roubos@tudelft.nl

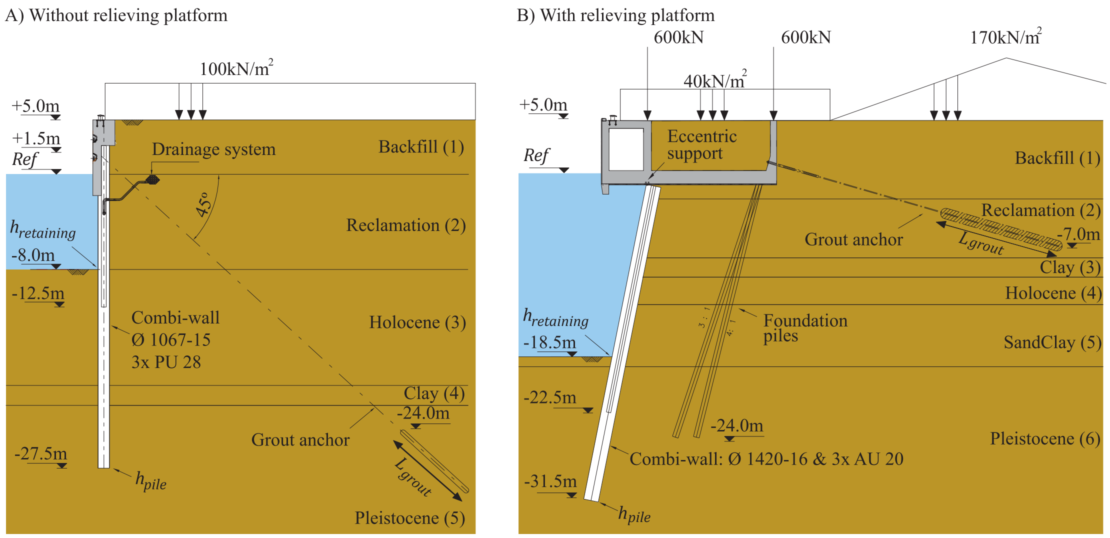

Figure 1. Cross-section of the reference quay walls without (A) and with (B) a relieving platform, located in the port of Rotterdam.

assessments of a quay wall without (Figure 1(A)) and with a relieving platform (Figure 1(B)). Further structural information can be found in Appendix 1. The failure modes were evaluated on the basis of limit state functions (Section 2.2).

Both quay walls have been built in practice and have been equipped with sensors. They were modelled with the hardening soil constitutive model to represent the soils' stress–strain behaviour, which takes into account the stress dependency of soil stiffness. The reader is referred to Appendix 1 for further details regarding the dimensions and numerical mesh used. The calculation output of the finite element models used has been compared to the monitoring data (Adel 2018; Berg et al. 2018) and to the results of the original design (Timmermans 2017; Eijk 2011). The stochastic variables considered are described in Section 2.3. The reliability interface developed enables the use of customised limit state functions and includes new options and features such as the possibility to account for uncertainty in water levels and geometry. It controls both the input and the output for the finite element model via "remote scripting" and the settings of the selected reliability method (Figure 2).

Most of the calculations were performed using the Abdo-Rackwitz *FORM* algorithm (Abdo and Rackwitz 1991) since this algorithm is able to take into account a large number of stochastic variables. The settings used are described in (Roubos 2019). Since coupling a finite element model with a reliability method can easily become a "black box", the outcomes were evaluated. This was done by performing reliability-based assessments using an alternative reliability tool while analytically modelling the quay wall using Blum's method (Blum 1931), which was commonly used until the end of the twentieth century to design all quay walls in Rotterdam. The Blum-based probabilistic analysis was performed on the basis of the Rackwitz-Fiessler *FORM* algorithm (Rackwitz and Fiessler 1997), and a more computational extensive crude Monte Carlo analysis (Roubos et al. 2020). Since some variables are correlated, Section 2.4 presents the method used to determine partial factors of safety for correlated stochastic variables.

2.2. Main failure modes and limit state functions

Failures of quay walls can be categorised into different failure modes, and hence multiple limit states have to be evaluated. This study evaluates the most relevant limit state functions of the failure modes in terms of reliability (Figure 3); it does not extend to evaluation of the entire system of failure modes, but rather focuses on the reliability index of individual structural components or failure modes in accordance with the Eurocode approach (NEN-EN 1990, 2011). Basic performance measures of reliability-based assessments are typically expressed as a probability of failure P_f on the basis of the limit state function (LSF) $Z = g(x) = 0$ (JCSS 2001). The failure probability P_f is defined as outcrossing $g(x) = 0$, and is generally directly related to the reliability index β (Cornell 1969; Hasofer and Lind 1974).

The limit state for yielding (Figure 3(A)) in the outer fibres of the combi-wall was evaluated using Equation (1). In addition, the calculation output of the finite element model – such as bending moments, axial forces, anchor forces and ΣMsf – was subjected to model

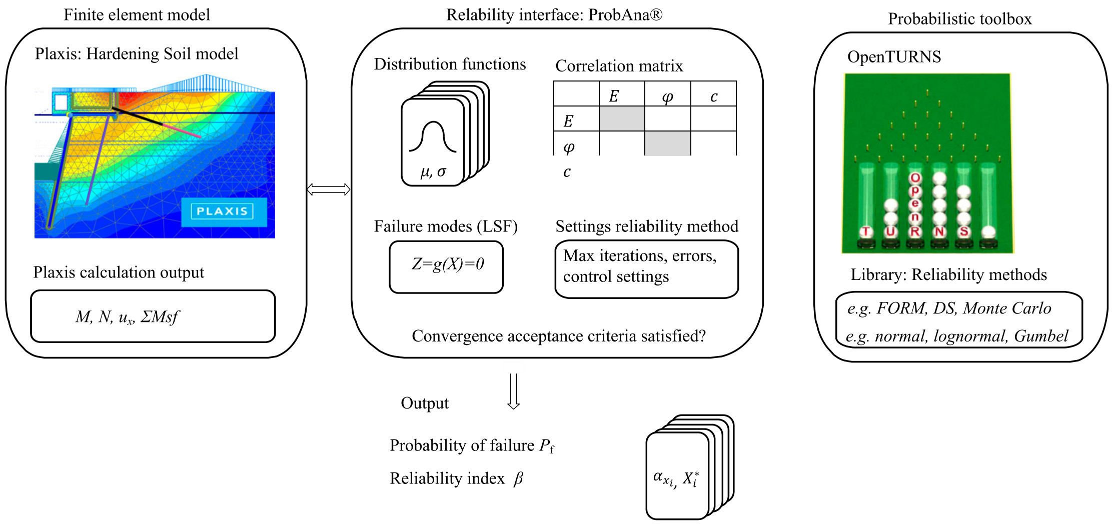

Figure 2. Reliability interface coupling the finite element software Plaxis with the probabilistic toolbox OpenTURNS.

uncertainty by introducing θ_M, θ_N, θ_F, and θ_{Msf}, respectively.

$$Z_{STR;yield}(z) = f_y - \max\left(\frac{\theta_M M_{wall}(z)}{W_{wall}} + \frac{\theta_N N_{tube}(z)}{A_{tube}}\right) \quad (1)$$

where $Z_{STR;yield}$ is the state function of maximum stress in the combi-wall (kN/m^2), f_y is the yield strength (kN/m^2), M_{wall} is the bending moment in combi-wall (kNm/m), N_{tube} is the axial force in combi-wall (kNm/m), W_{wall} is the section modulus, combi-wall (m^3/m), A_{tube} is the sectional area of tube (m^2/m), z is the depth across height of combi-wall (m), θ_M is the factor to account for model uncertainty for bending moments (-), θ_N is the factor to account for model uncertainty for axial forces (-).

The structural (Figure 3(B)) and the geotechnical limit states (Figure 3(C)) of the anchors were evaluated using Equations (2) and (3), respectively. The strength of the grout body depends largely on the factor α_t,

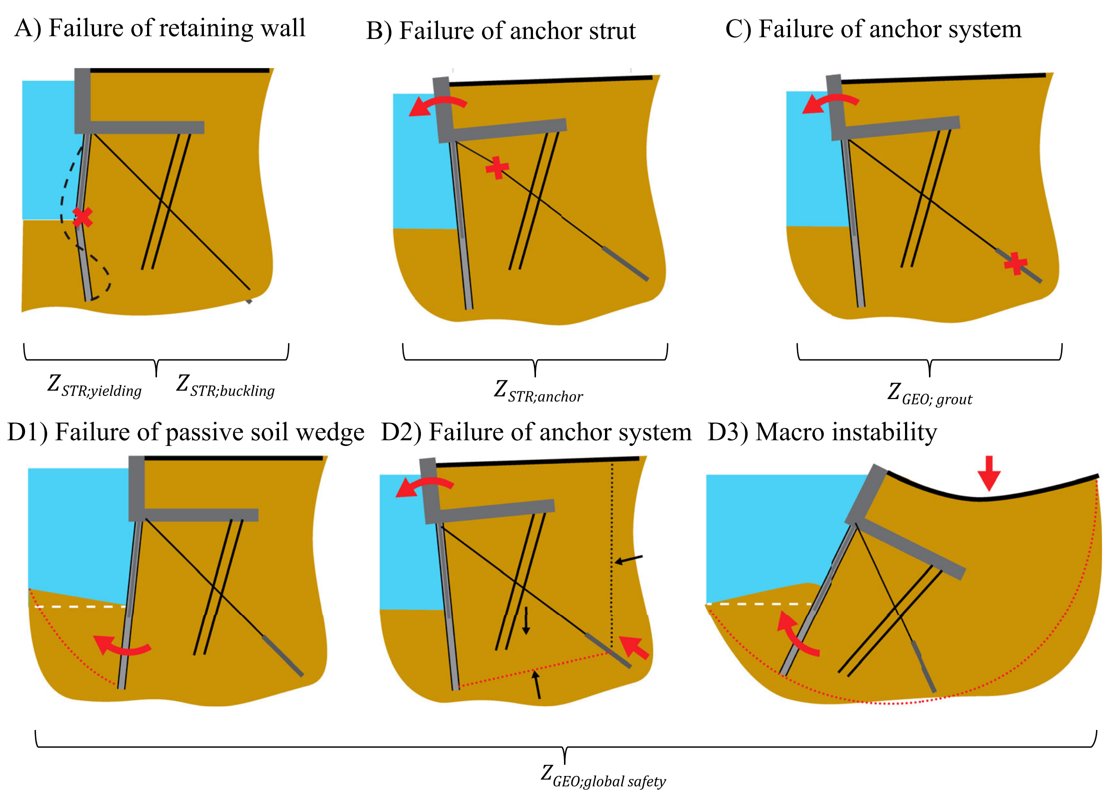

Figure 3. Failure modes of quay walls considered in this study.

which represents the shear capacity along the grout body.

$$Z_{STR;anchor} = f_y - \frac{\theta_F F_{anchor}}{A_{anchor}} \quad (2)$$

$$Z_{GEO;grout} = \alpha_t O_A L_A q_c - \theta_F F_{\mathrm{anchor}} \quad (3)$$

where $Z_{STR;anchor}$ is the state function of maximum stress in cross-section anchor strut (kN/m^2), $Z_{GEO;grout}$ is the state function of capacity of grout body anchor system (kN), F_{anchor} is the anchor force (kN), A_{anchor} is the sectional area of anchor strut (m^2), α_t is the tension capacity factor of grout body (-), O_A is the circumference of grout body (m), q_c is the cone penetration resistance (MPa), L_A is the length of grout body (m), θ_N is the factor to account for model uncertainty for axial forces (-), θ_F is the factor to account for model uncertainty for anchor forces (-).

Furthermore, the limit state function $Z_{GEO;global}$ covers all geotechnical failure modes (Figure 3(D)) simultaneously and is defined as:

$$Z_{GEO;global} = 1.0 - \theta_{Msf}\Sigma Msf = 1 - \theta_{Msf}\frac{c' + \sigma_n \tan(\varphi')}{c'_{reduced} + \sigma_n \tan(\varphi'_{reduced})} \quad (4)$$

where $Z_{GEO;global}$ is the state function of global safety factor (-), ΣMsf is the Global stability ratio related to φ-c reduction. The friction angle φ' and cohesion c' are successively decreased until geotechnical failure occurs (-), θ_{Msf} is the factor to account for model uncertainty for global stability ratio (-).

2.3. Distribution functions and correlations

This section presents the type of probability distribution function and the variation coefficients for each stochastic variable used in this study (Appendix 2), which can significantly affect the outcome of reliability-based assessments (Rackwitz 2000). The marginals of the distribution functions are based on the characteristic values used in the original design. By contrast, the type of distribution function was determined in accordance with recommendations found in literature, but predominantly on the basis of the Probabilistic Model Code (JCSS 2001).

2.3.1. Material properties X_i

The background documents for NEN-EN 1997 (2004) show that the low characteristic value of soil strength φ or c and soil stiffness E_{50} commonly represents a 5% fractile, while the recommendations for weight density γ_{sat} typically represent the expected value. Since previous studies have shown that the variability in soil strength is a dominant source of uncertainty and that the variation coefficient in the literature varies widely (Cherubini 1999; Das and Das 2010; ISO 2394 2015; Schweckendiek et al. 2012; Teixeira et al. 2016; Wolters, Bakker, and Gijt 2012) its influence was investigated by performing a sensitivity analysis (Section 3.3). Furthermore, the angle of internal friction depends on the strain rate. In this study, the reference calculation was based on $V_{x;\varphi}$=0.1, considered at 5% strain rate (Lindenberg 2008), which is in accordance with the original design.

2.3.2. Loads F_i

The variable loads represent the lifetime maxima for a reference period of 50 years and are determined using the Gumbel extreme value distribution function. The characteristic value of terminal loads is generally determined by an operational limit, whereas characteristic wind-induced crane loads typically represent a return period, e.g. T_R=50 years. In accordance with the design report, the characteristic value of the outer water level equals the mean value of the "low low water" spring tide level, which seems acceptable because waterhead differences are not the dominant load. Furthermore, the corresponding groundwater table is largely influenced by the presence of the drainage system. Analogous with NEN-EN 1997 (2004), the outer water and groundwater levels were considered to be a geometric variable.

2.3.3. Geometric variable a_i

The variation coefficients of structural dimensions such as t_{tube} and D_{tube}, were determined taking into account execution tolerances and project-specific acceptance criteria, which in Rotterdam are slightly stricter than the recommendations in the Probabilistic Model Code (JCSS 2001) and NEN-EN 10029 (2010). In this study, geometrical variations such as variation in retaining height, installation depth and the length of the grout body were taken into account. Initially, geological variations in soil deposition were distinguished. Their geometrical standard deviations were initially set at Δ_a=0.35 m in order to investigate whether geological variations in soil-layer thickness are relevant. This appeared not to be the case, and consequently the standard deviations were not investigated further.

2.3.4. Model uncertainty θ_i

In this study, a stochastic model factor was applied to the calculation output (Section 2.2). A variation coefficient of 0.1 was used, which seems a reasonable value. Since experiments are lacking, the influence of model uncertainty on the reliability index was investigated by performing a sensitivity analysis (Section 3.3).

Table 1. Simplified correlation matrix.

	E_{50}	φ	γ_{sat}	c'	h_{OWL}	h_{GWL}
E_{50}	-	0.25[a]	0.50[a]	0.12[a]	-	-
φ	0.25[a]	-	0.50[a]	−0.65[a]	-	-
γ_{sat}	0.50[a]	0.50[a]	-	−0.09[a]	-	-
c'	0.12[a]	−0.65[a]	−0.09[a]	-	-	-
h_{OWL}	-	-	-	-	-	0.75[b]
h_{GWL}	-	-	-	-	0.75[b]	-

[a]Based on a statistical analysis of a large dataset in Rotterdam (Wolters, Bakker, and Gijt 2012).
[b]Approximated on the basis of statistical examination of the waterhead difference of a quay wall equipped with sensors in the port of Rotterdam (Well 2018). This correlation is only valid when waterhead differences are non-dominant loads.

2.3.5 . Correlation matrix

The dependency between stochastic variables was taken into account to accurately estimate the probability of failure. Correlations between soil parameters were determined statistically by analysing a relatively large database, including the data from site investigations of several projects adjacent to the reference quay walls (Wolters, Bakker, and Gijt 2012), which align with other literature (Teixeira et al. 2016). Table 1 presents the correlation matrix used in this study. The unsaturated (γ_{dr}) and saturated soil-weight densities (γ_{sat}) were assumed to be fully dependent; likewise, the elastic unloading (E_{ur}) and reloading moduli (E_{oed}) were considered to be fully dependent on the soil stiffness E_{50}. These correlations were implemented implicitly in the model by applying a constant deterministic difference or ratio between the variables in order to reduce the number of stochastic variables and hence minimise the calculation effort. The same approach was undertaken to correlate the two vertical crane loads (F_{crane}).

2.4. Derivation of sensitivity and partial factors in the event of correlations

This section describes the derivation of the sensitivity factors and the partial factors of safety, taking into account correlations between some dominant stochastic variables. In the event that input variables are correlated, the input sequence of correlated random variables in a *FORM* approximation influence the sensitivity factors of the uncorrelated normal space α_u found. In order to correctly highlight the contribution of a model parameter to the reliability index obtained, this paper presents the sensitivity factors of the correlated normal space, denoted as α_y.

The reliability index β found generally does not exactly match the reliability target β_t. In order to compare the results from this study with the partial factors used in the original design, it was therefore necessary to slightly scale the reliability index. Since some input variables are correlated, the Cholesky decomposition (Jiang, Basudhar, and Missoum 2011; Lemaire 2009; Melchers and Beck 2018) was used directly to transform the results from the standard space U to the physical space X. The partial factors of the scaled design values x_i^* were derived using Equation (5). It should, however, be noted that this equation does not yet account for model uncertainties. Section 4.2 further discusses how model uncertainty can be taken into consideration.

$$\gamma_{m;i} = \frac{X_{k;i}}{X_{d;i}} \text{and } \gamma_{f;i} = \frac{F_{d;i}}{F_{k};\, i} \quad (5)$$

where: $\gamma_{f;i}$ is the partial factor for load i, without accounting for model uncertainties (-), $\gamma_{m;i}$ is the partial factor for material property i, without accounting for model uncertainties (-), $X_{d;i}$ is the design value for material property i, $X_{k;i}$ is the characteristic for material property i, $F_{d;i}$ is the design value load i, $F_{k;i}$ is the characteristic value load i.

3. Results

3.1. Evaluation of Abdo–Rackwitz algorithm outcomes

Since coupling a reliability method to a finite element model can become a black box, its outcomes were compared with the results of other reliability methods and tools using Blum's analytical method (Section 2.1). In this study, the comparison was made for the structural limit state Z_{yield} of the quay wall without the relieving platform. This is because Z_{yield} can also be modelled using Blum's method. The differences found appear to be fairly small (Table 2), and hence performing a finite element-based reliability assessment using the Abdo-Rackwitz algorithm seems a reasonable approach. Section 4.1 further discusses its performance.

3.2. Results of finite element-based reliability assessments

The reliability indices obtained for the two reference quay walls, without and with a relieving platform, are listed in Table 3. This table shows that, when model uncertainty and correlations are taken into account, the reliability index decreases. The reliability indices found differ per failure mode, indicating that only some structural components or failure modes are close to the target reliability index of RC2, which equals 3.8. The results are further discussed in Section 4.1.

Since some stochastic variables are correlated, the sensitivity factors $\alpha_{y;i}$, provide the most accurate description of their contribution to the reliability index found (Section 2.4). Table 4 includes the sensitivity factors α_y taking model uncertainty into account, and only lists the values

Table 2. Comparison of lifetime reliability indices found using finite element-based and Blum-based reliability assessment for Z_{yield} of the quay wall without a relieving platform.

Design model		Reliability toolbox	Reliability method	Algorithm	Z_{yield}
Plaxis	Finite elements	ProbAna®[a] +OpenTURNS[b]	*FORM*	Abdo and Rackwitz (1991)	3.76[c]
Blum	Analytical	Prob2B®[d]	*FORM*	Rackwitz and Fiessler (1997)	3.87[c,e]
Blum	Analytical	Matlab	Crude Monte Carlo	n/a	3.77[e]

[a]The reader is referred to Laera and Brinkgreve (2017) for further details.
[b]The reader is referred to Andrianov et al. (2007) for further details.
[c]The associated design point and sensitivity factors are listed in Appendix 3.
[d]The reader is referred to (Courage and Steenbergen 2007) for further details.
[e]The reader is referred to Roubos et al. (2020) for further details.

Table 3. Lifetime reliability index β for the two reference quay walls for the different limit state functions, with and without taking into account correlations and model uncertainty θ.

		Without relieving platform				With relieving platform			
Correlations	Model uncertainty	Z_{yield}	Z_{strut}	Z_{grout}	Z_{GEO}	Z_{yield}	Z_{strut}	Z_{grout}	Z_{GEO}
Yes	Yes (V=0.1)	3.76	5.43[a]	4.51	5.54[a]	3.91	*n/a*[b]	*n/a*[b]	3.69
Yes	No	4.07	5.54[a]	5.12[a]	7.00[a, c]	4.32	*n/a*[b]	*n/a*[b]	4.49
No	No	4.51	5.80[a]	5.14[a]	7.62[a, c]	6.68[a, c]	*n/a*[b]	*n/a*[b]	4.84

[a]The probability of failure of this limit state is quite low. It should be noted that the accuracy of *FORM* beyond a reliability index of 5 is not guaranteed. This is considered to be actable since these failure modes are not likely to occur in reality.
[b]It was not possible to locate the design point, since soil failure occurred in the hardening soil model.
[c]Beyond accuracy of *FORM*.

higher than 0.1. A high factor indicates that the variability in a model parameter contributes significantly to the probability of failure. Although the sensitivity factors can differ substantially per limit state function, the properties of the soil layers which largely influence the active and passive earth pressure acting on the quay wall are relatively influential, whereas the other soil layers show much lower sensitivity factors. Furthermore, uncertainty related to model uncertainty seems to play an important role. According to the sensitivity factors in Table 4, time-dependent random variables such as loads and water levels have quite low sensitivity factors and hence the reliability problem seems largely dominated by uncertainty in time-independent random variables, such as soil and grout properties. In addition, the limit state functions of the quay wall with the relieving platform are completely dominated by the uncertainty about the soil properties of one specific soil layer, i.e. the Pleistocene sand.

3.3. Sensitivity analysis

The aim of the sensitivity analysis was to show the extent to which reliability indices are influenced by small variations in random variables. This section predominantly presents the results found for the limit state Z_{yield}. This is because this limit state is well-known, its outcomes are close to the reliability targets and it has been widely considered in other studies, which helps us to interpret the results obtained in this one. In accordance with other literature (Section 2.3), Figure 4 shows that small changes in the variation coefficient of the soils' internal friction angle φ substantially influence the reliability index of Z_{yield} for both reference quay walls. The effect of the friction angle on the reliability index of the geotechnical limit states Z_{GEO} is generally even higher. Since the soil properties of the Pleistocene sand are quite dominant for the quay wall with a relieving platform, changing the type of distribution of its internal friction angle has more impact than changing the type of distribution functions of the quay wall without a relieving platform. Furthermore, Figure 4 shows that neither changing the variation coefficient of the non-dominant loads nor their distribution function makes much of a difference for either reference quay wall. In addition, Table 5 shows that slightly changing the variation coefficients of θ_M and $\theta_{\Sigma Msf}$ can also have a fairly high impact on the reliability index obtained.

During the service life of a quay wall, port authorities or terminals frequently ask to enhance its functionality by, for example, deepening the berth or increasing operational loads. Figure 5 shows the effect of these functional changes on the reliability index and demonstrates that the reliability index is also significantly influenced by changing functional requirements, while maintaining the same variation coefficient. Hence, a calculated reliability index is always relative to a certain functionality, as further discussed in Section 4.1.

3.4. Results: partial factors of safety

When sensitivity factors are used to derive partial factors, they should ideally be based on several *FORM*-based

Table 4. Sensitivity factors α_y >0.1 for the two reference quay walls, taking into account correlations and model uncertainties.

Random variable		Without relieving platform				With relieving platform	
limit state		Z_{yield}	Z_{strut}	Z_{grout}	Z_{GEO}	Z_{yield}	Z_{GEO}
Reliability index β	Time-dependent	3.76	5.43[a]	4.51	5.54[a]	3.91	3.69
Materials X_i							
$E_{50;Backfill}$	No						
$E_{50;Clay}$	No						
$E_{50;\ Holocene}$	No	−0.24	−0.25	−0.10	−0.14		
$E_{50;\ Reclamation}$	No	−0.17		−0.10			
$E_{50;SandClay}$	No	n/a	n/a	n/a	n/a		
$E_{50;Pleistocene}$	No					−0.31	−0.24
$\varphi_{Backfill}$	No			−0.18			
φ_{Clay}	No						
$\varphi_{Holocene}$	No	−0.44	−0.72	−0.18	−0.31		
$\varphi_{Reclamation}$	No	−0.36	−0.23	−0.21			
$\varphi_{SandClay}$	No	n/a	n/a	n/a	n/a		
$\varphi_{Pleistocene}$	No				−0.40	−0.76	−0.67
$\gamma_{sat;Backfill}$	No		−0.11				
$\gamma_{sat;Clay}$	No						
$\gamma_{sat;Holocene}$	No	−0.34	−0.50	−0.14	−0.32		
$\gamma_{sat;Reclamation}$	No	0.18		0.12			
$\gamma_{sat;SandClay}$	No	n/a	n/a	n/a	n/a		
$\gamma_{sat;Pleistocene}$	No				−0.21	−0.51	−0.46
c_{Clay}	No						
$c_{SandClay}$	No	n/a	n/a	n/a			
$f_{y;combi\text{-}wall}$[b]	No	−0.19	n/a	n/a	n/a		n/a
$f_{y;anchor}$[b]	No	n/a	−0.13	n/a	n/a	n/a	n/a
a_t	No	n/a	n/a	−0.55	n/a	n/a	n/a
q_c	No	n/a	n/a	−0.55	n/a	n/a	n/a
Loads F_i							
$Q_{surcharge}$	Yes	0.13	0.16	0.13		n/a	n/a
Q_{bulk}	Yes	n/a	n/a	n/a	n/a		
$F_{bollard}$	Yes					n/a	n/a
F_{crane}	Yes	n/a	n/a	n/a	n/a		
Geometry a_i							
h_{OWL}	Yes						
h_{GWL}	Yes						
h_{pile}[b]	No					−0.16	−0.15
$h_{retaining}$	No	−0.18	−0.13	−0.13			
t_{tube}[b]	No	−0.16					
D_{tube}[b]	No	−0.21	−0.10				
O_{grout}[b]	No	n/a	n/a	−0.17	n/a	n/a	n/a
L_{grout}[b]	No	n/a	n/a	−0.17	n/a	n/a	n/a
Model uncertainty θ_i							
θ_B	No	n/a	n/a	n/a	n/a	n/a	n/a
θ_M	No	0.42	n/a	n/a	n/a		n/a
θ_N; θ_F	No			0.35	n/a		n/a
$\theta_{\Sigma MSF}$	No	n/a	n/a	n/a	−0.74	n/a	−0.49

[a]The probability of failure of this limit state is quite low. It should be noted that the accuracy of *FORM* beyond a reliability index of 5 is not guaranteed. This is considered to be actable since these failure modes are not likely to occur in reality.
[b]Quality control procedures were taken into consideration.

assessments, the design points of which align with the required target reliability index. Table 3 shows that only some limit states are close to the reliability target β_t=3.8 of reliability class RC2 (NEN-EN 1990, 2011). Table 6 presents the partial factors related to the limit state Z_{yield} of both reference quay walls, as well as Z_{GEO} of the quay wall equipped with the relieving platform. The material factors $\gamma_{m;i}$ lower than 1 indicate that the design values of the non-dominant soil layers are lower than their characteristic values, but they are still higher than their mean value. Furthermore, the partial factor for the internal friction angle of the Pleistocene sand for the quay wall with the relieving platform is fairly high: approximately 1.3. This can be explained by the dominance of this specific soil layer, for which presumably an unrealistic combination of high strength properties and a high variation coefficient was assumed (Section 4), introducing an unrealistically low design value for $\varphi_{Pleistocene}$. The differences in sensitivity factors between the quay wall with and without a relieving platform can be explained by the difference in the number of dominant soil layers. In addition, fairly low partial load factors $\gamma_{f;i}$ were found; most were in the order of 1.1. Table 6 also shows that the model factor applied to the bending moments has much more influence than applying a model factor to the normal forces for Z_{yield}, being

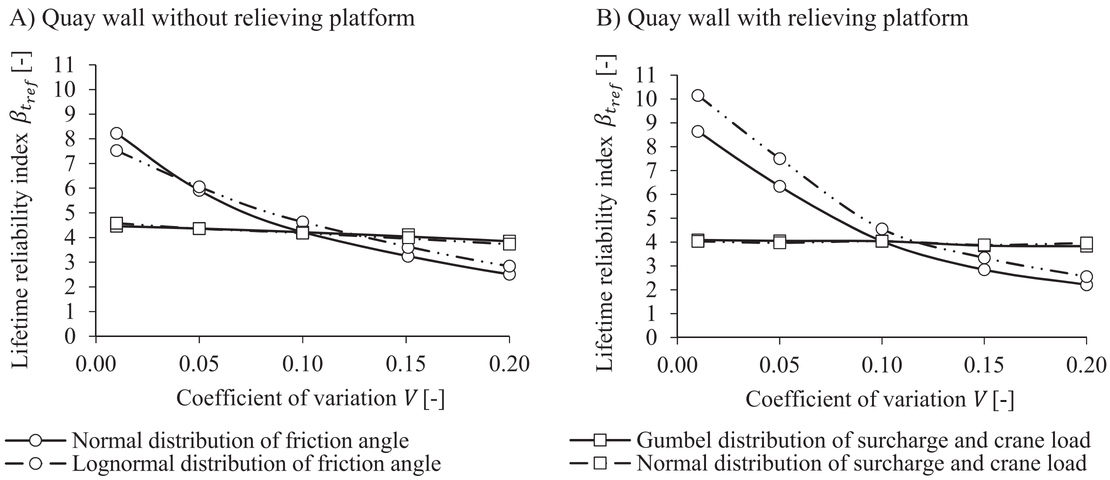

Figure 4. Influence of angle of internal friction φ' and live load Q on Z_{yield} for the reference quay wall without (A) and with (B) a relieving platform.

approximately 1.15 for the quay wall without the relieving platform, whereas $\theta_{\Sigma MSF}$ significantly influences Z_{GEO}.

4. Discussion

4.1. Evaluation of results

4.1.1. Robustness and efficiency of the Abdo–Rackwitz algorithm

The reliability methods available in OpenTURNS were compared in terms of efficiency, robustness and accuracy. Performing finite element-based reliability assessments using the Abdo-Rackwitz *FORM* algorithm appeared to be quite efficient; in particular, convergence is more efficient in this case than with the gradient-free Cobyla algorithm (Powell 1994), especially when many stochastic variables are taken into consideration. In general, roughly between two and ten iterations were needed to satisfy the convergence acceptance criteria. The one exception was the limit state function Z_{GEO}, for which the calculation time per evaluation and the number of iterations required were approximately a factor of four higher (Table 7). This was caused mainly by the presence of higher numerical noise in the global stability ratio ΣMsf. Using an appropriate finite difference step size ε (Roubos 2019) and robust numerical control settings for the hardening soil solver were crucial to achieve convergence (Laera and Brinkgreve 2017).

Table 5. Influence of variation coefficient V_θ on Z_{yield} and Z_{GEO} for the quay wall without a relieving platform.

Limit state	Description	Variation coefficient V θ_M	θ_N	$\theta_{\Sigma Msf}$	Lifetime reliability index β
Z_{yield}	Reference calculation	0.10	0.10	n/a	3.76
Z_{yield}	Recommended values for "frames" (JCSS 2001)	0.20	0.10	n/a	3.06
Z_{yield}	Recommended values for "plates" (JCSS 2001)	0.10	0.05	n/a	3.83
Z_{GEO}	Reference calculation	n/a	n/a	0.10	5.54
Z_{GEO}	Slightly lower variation coefficient	n/a	n/a	0.05	6.83

4.1.2. Comparison with original design

The results of the finite element-based reliability assessments correspond fairly well with the original design, which requires a minimum reliability index of 3.8 for structural members to comply with the Eurocode standard (Gijt and Broeken 2013). Due to bearing capacity requirements, both quay walls have a relatively large installation depth. Consequently, the quay wall without a relieving platform has some margin in its geotechnical capacity (Z_{GEO}), whereas this is not the case for the quay wall with a relieving platform. In addition, the anchor systems (Z_{strut} and Z_{grout}) seem to be quite safe. The main reasons for this appear to be the low uncertainties due to the observance of strict test protocols and the fact that the original design takes into account failure of the neighbouring anchors. Taking correlations and model uncertainty into account, a target reliability index of 3.76 for Z_{yield} was found for the quay wall without the relieving platform (Table 3). This is close to the target reliability index of 3.8. The reliability indices obtained for Z_{yield} and Z_{GEO} of the quay wall with a relieving platform were 3.91 and 3.69 respectively (Table 3), which are also fairly close to the reliability target. It should, however, be noted that extremely low design values for soil strength were sometimes obtained for Z_{yield}, – for example, for the angle of internal friction of the Pleistocene sand.

4.1.3. Internal friction angle of soil

The reliability indices found are considered to be somewhat conservative, mainly because the reliability

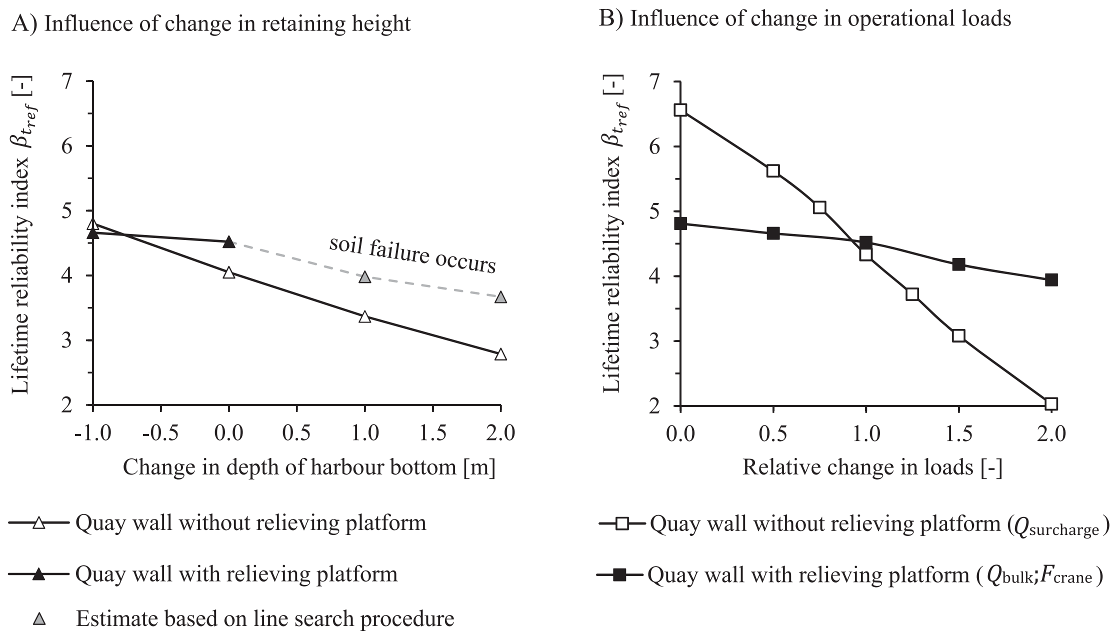

Figure 5. Influence of deepening the harbour bottom (A) and changing the surcharge load (B) on the structural limit state Z_{yield}.

index is quite sensitive to changes in the variation coefficient of the internal friction angle of soil (Figure 4). Interestingly, a previous study by Huijzer and Hannink (1995) indicates that the mean value of the friction angle rises in line with an increasing soil deformation/strain rate, whereas the associated standard deviation decreases. The variation coefficient is therefore lower for soils with higher strength properties. This was also found by Cherubini (1999). In this study, the variation coefficient of soil strength was assumed to be 0.1 for all soil layers, in accordance with NEN-EN 1997 (2004), although Huijzer (1996) showed that the coefficient of variation of the sand layers in the Maasvlakte area of the port of Rotterdam is in the range 0.03-0.07, which would result in a much higher reliability index (Figure 4).

4.1.4. Geometrical variations in soil layers

It was also found that the variation in soil-layer thickness had a negligible influence on the reliability index. Consequently, there seems to be no direct need to consider soil-layer thickness as a random variable when performing reliability-based assessments of soil-retaining walls with similar soil stratigraphy. This significantly reduces the number of model parameters, and hence the required calculation time. When we reduce the sand layers of the quay wall without the relieving platform – since they are fairly thick – by 50%, the reliability index for Z_{yield} increases accordingly, from 4.07 to 4.55. This addresses the added value of soil investigation as well as site-specific knowledge.

4.2. Evaluation and derivation of partial factors of safety

This section reflects upon the partial factors used in quay-wall engineering and discusses how correlations and model uncertainty influence the derivation of partial factors of safety. Before comparing and deriving partial factors, it must be clear how model uncertainty can be taken into account.

4.2.1. Options for implementation of model uncertainty

In accordance with NEN-EN 1990 (2011), a design is considered to be sufficiently safe if the design value of the resistance R_d is higher than the design value of the action effect E_d. These two values are defined as:

$$E_d = E(F_{d;i}, a_{d;i}, \theta_{d;i}) \tag{6}$$

$$R_d = R(X_{d;i}, a_{d;i}, \theta_{d;i}) \tag{7}$$

where E_d is the design value of action effect, E is the action effect, R_d is the design value of resistance, R is the resistance, $F_{d;i}$ is the design value of load i, $X_{d;i}$ is the design value of material property i, $a_{d;i}$ is the design value of geometric property i, $\theta_{d;i}$ is the design value of model uncertainty i.

In quay-wall engineering, however, material properties of soil layers – such as soil strength and weight density – can act simultaneously as resistance and load. Hence, the definition of the action effect must be reformulated as $E_d = E(F_{d;i}, X_{d;i}, a_{d;i}, \theta_{d;i})$. When deriving partial factors, two approaches can generally be distinguished:

Table 6. Load and material factors for a fixed target reliability index, β=3.8, assuming that α_u is invariant and taking into account correlations.

Random variable limit state	Characteristic values	Quay wall without relieving platform		Quay wall with relieving platform			
		Z_{yield} with θ	Z_{yield} without θ	Z_{yield} with θ	Z_{yield} without θ	Z_{GEO} with θ	Z_{GEO} without θ
Material properties	X_k	$\gamma_{m;i}$	$\gamma_{m;i}$	$\gamma_{m;i}$	$\gamma_{m;i}$	$\gamma_{m;i}$	$\gamma_{m;i}$
$E_{50;Backfill}$	$X_{5\%}$	0.71	0.73	0.71	0.70	0.72	0.69
$E_{50;Clay}$	$X_{5\%}$	0.74	0.75	0.72	0.71	0.71	0.72
$E_{50;\ Holocene}$	$X_{5\%}$	0.90	0.97	0.73	0.72	0.72	0.69
$E_{50;\ Reclamation}$	$X_{5\%}$	0.84	0.82	0.69	0.70	0.72	0.71
$E_{50;SandClay}$	$X_{5\%}$	n/a	n/a	0.75	0.74	0.72	0.72
$E_{50;Pleistocene}$	$X_{5\%}$	0.73	0.74	1.01	1.04	0.91	0.90
$\varphi_{\ Backfill}$	$X_{5\%}$	0.82	0.82	0.84	0.84	0.85	0.80
$\varphi_{\ Clay}$	$X_{5\%}$	0.84	0.85	0.84	0.83	0.82	0.80
$\varphi_{\ Holocene}$	$X_{5\%}$	1.03	1.15	0.85	0.85	0.85	0.82
$\varphi_{\ Reclamation}$	$X_{5\%}$	0.99	0.97	0.83	0.78	0.84	0.84
$\varphi_{\ SandClay}$	$X_{5\%}$	n/a	n/a	0.87	0.88	0.86	0.84
$\varphi_{\ Pleistocene}$	$X_{5\%}$	0.83	0.84	1.29	1.28	1.19	1.26
$\gamma_{sat;\ Backfill}$	µ	0.98	0.99	0.99	0.99	1.00	0.98
$\gamma_{sat;\ Clay}$	µ	1.01	1.01	1.00	1.00	0.99	1.00
$\gamma_{sat;\ Holocene}$	µ	1.04	1.07	1.00	1.00	1.00	0.99
$\gamma_{sat;\ Reclamation}$	µ	1.04	1.06	0.99	0.99	1.00	0.99
$\gamma_{sat;\ SandClay}$	µ	n/a	n/a	1.01	1.02	1.00	0.99
$\gamma_{sat;\ Pleistocene}$	µ	1.00	1.00	1.14	1.19	1.11	1.13
c_{Clay}	$X_{5\%}$	0.72	0.74	0.78	0.75	0.69	0.74
$c_{SandClay}$	$X_{5\%}$	n/a	n/a	0.75	0.74	0.75	0.94
$f_{y;CombiWall}$ [a]	$X_{5\%}$	1.01	0.97	0.95	0.95	n/a	n/a
Loads	F_k	$\gamma_{f;i}$	$\gamma_{f;i}$	$\gamma_{f;i}$	$\gamma_{f;i}$	$\gamma_{f;i}$	$\gamma_{f;i}$
$Q_{surcharge}$	Nominal	1.11	1.12	n/a	n/a	n/a	n/a
Q_{bulk}	Nominal	n/a	n/a	1.06	1.06	1.06	1.07
F_{crane}	Nominal	n/a	n/a	1.07	1.05	1.05	1.05
$F_{bollard}$	$X_{95\%}$	1.06	1.06	n/a	n/a	n/a	n/a
Geometry	$\Delta_{a;k}$	$\Delta_{a;i}$	$\Delta_{a;i}$	$\Delta_{a;i}$	$\Delta_{a;i}$	$\Delta_{a;i}$	$\Delta_{a;i}$
h_{OWL}	LLWS[b]	0.00m[c]	−0.02m[c]	−0.01m[c]	0.00m[c]	0.00m[c]	−0.04m[c]
h_{GWL}	$h_{drainage}$+0.3m	0.04m[c]	0.01m[c]	−0.01m[c]	0.00m[c]	0.00m[c]	0.06m[c]
h_{pile} [a]	µ	−0.01m[c]	−0.01m[c]	−0.04m[c]	−0.20m[c]	−0.22m[c]	−0.17m[c]
$h_{retaining}$ [d]	µ	−0.26m[c]	−0.29m[c]	−0.25m[c]	−0.10m[c]	−0.06m[c]	−0.10m[c]
t_{tube} [a]	µ	−0.05cm[c]	−0.06cm[c]	−0.01cm[c]	−0.01cm[c]	0.00cm[c]	0.00cm[c]
D_{tube} [a]	µ	0.00cm[c]	0.00cm[c]	0.92cm[c]	0.32cm[c]	0.01cm[c]	0.27cm[c]
Model uncertainty		$\gamma_{\theta;i}$	$\gamma_{\theta;i}$	$\gamma_{\theta;i}$	$\gamma_{\theta;i}$	$\gamma_{\theta;i}$	$\gamma_{\theta;i}$
θ_M	µ	1.14	n/a	1.04	n/a	n/a	n/a
θ_N	µ	1.04	n/a	1.02	n/a	n/a	n/a
$\theta_{\Sigma MSF}$	µ	n/a	n/a	n/a	n/a	0.82	n/a

[a]Quality-control procedures were taken into consideration.
[b]Low low water level at spring tide (Gijt and Broeken 2013).
[c]Geometrical change Δ_a in metres, which is added to the characteristic geometrical variable to obtain the design value.
[d]Scour was not taken into consideration.

either model factors γ_{Sd} and γ_{Rd} can be applied to the representative load and resistance effect respectively (Equations (8) and (9)) or model factors γ_{Sd} and γ_{Rd} can be applied directly to individual load and resistance parameters using γ_f and γ_m respectively (Equations (10) and (11)).

$$E_d = \gamma_{Sd} E\left(\gamma_f F_{rep;i}, \frac{X_{rep;i}}{\gamma_m}, a_{d;i}\right) \tag{8}$$

$$R_d = \frac{R\left(\frac{X_{rep;i}}{\gamma_m}, a_{d;i}\right)}{\gamma_{Rd}} \tag{9}$$

or

$$E_d = E\left(\gamma_F F_{rep;i}, \frac{X_{rep;i}}{\gamma_M}, a_{d;i}\right) \tag{10}$$

$$R_d = R\left(\frac{X_{rep;i}}{\gamma_M}, a_{d;i}\right) \tag{11}$$

Table 7. Efficiency of the Abdo-Rackwitz algorithm.

	Without relieving platform				With relieving platform	
Limit state	Z_{yield}	Z_{strut}	Z_{grout}	Z_{GEO}	Z_{yield}	Z_{GEO}
Reliability index	3.76	5.43	4.51	5.54	3.91	3.69
Number of variables	27	26	29	25	31	29
Iteration	2	9	3	n/a[a]	2	n/a[a]
Limit state evaluations	104	510	179	n/a[a]	127	n/a[a]
Residual error[b]	<<0.1	<<0.1	<<0.1	<<0.1	<<0.1	<<0.1
Constraint error[b]	<1%	<2%	<0.5%	<2.5%	<2%	<1%

[a]An alternative starting point was used, since the reliability index was fairly low. This was found by only activating the dominate variables, after performing approximately 30 iterations.
[b]The reader is referred to Roubos (2019) for additional information.

Table 8. Partial factors γ_m and γ_q for Z_{yield} with and without correlations between soil conditions, for target reliability indices of 3.3, 3.8 and 4.3 respectively.

Model parameter			Eurocode standard[a]			Without correlations			With correlations		
Reliability class			RC1	RC2	RC3						
Reliability index	X_{rep}, F_{rep}	V	3.3	3.8	4.3	3.3[b]	3.8[b]	4.3[b]	3.3[b]	3.8[b]	4.3[b]
Correlations			No	No	No	No	No	No	Yes	Yes	Yes
Soil stiffness E_{50}	$X_{k;5\%}$	0.20	1.30	1.30	1.30	0.78[c]	0.79[c]	0.79[c]	0.94[c]	0.97[c,d]	1.01[c]
Tangent of friction angle φ	$X_{k;5\%}$	0.10	1.15	1.175	1.20	1.05[c]	1.10[c]	1.15[c]	1.11[c]	1.18[c,d]	1.25[c]
Weight density γ_{sat}	μ_X	0.05	1.00	1.00	1.00	0.97[c]	0.97[c]	0.97[c]	1.06[c]	1.07[c,d]	1.08[c]
Surcharge load Q	$F_{k;max}$[e]	0.01	1.23[f]	1.36[f]	1.50[f]	1.10	1.11	1.12	1.11	1.12[d]	1.13

[a]Based on NEN-EN 1990 (2011) and NEN-EN 9997 (2016).
[b]The target reliability index was scaled using the sensitivity factors in the U-space for Z_{yield}, associated with $\beta = 4.07$.
[c]Partial factor represents dominant Holocene sand layer and does not account for model uncertainty.
[d]See fourth column of Table 6.
[e]Operational limit as specified in service level agreement with the user.
[f]This partial factor does not include model uncertainty and represents γ_q, which was derived by dividing γ_Q by a model factor of 1.1 (NEN-EN 1990, 2011).

In which:

$$\gamma_F = \gamma_{Sd}\gamma_f \text{ and } \gamma_M = \gamma_{Rd}\gamma_m$$

where γ_f is the partial factor for actions (-), γ_F is the partial factor for actions, also accounting for model uncertainties (-), γ_m is the partial factor for material properties (-), γ_M is the partial factor for material properties, also accounting for model uncertainties (-), γ_{Sd} is the partial factor associated with uncertainties in the action or the action-effect model (-), γ_{Rd} is the partial factor associated with uncertainties in the resistance model (-).

4.2.2. Evaluation of partial factors used in the design without model uncertainty

When reflecting on the partial factors presently used, it is crucial to know if and how model uncertainty is accounted for in the design approach. The design manual (Gijt and Broeken 2013), show that no model factors are applied either to resistance or to action effects. If model uncertainty is accounted for in the design, it must be included in the partial load and material factors; that is, via γ_F and γ_M. It is, however, rather questionable whether γ_M includes model uncertainty; this is because the calibration report (Calle and Spierenburg 1991) reveals that correlations are not taken into consideration.

Since Z_{yield} was included in the calibration report and the reliability index for the quay wall without the relieving platform was found in this study to be close to the reliability target for RC2, this limit state was used to determine partial factors of safety. Let us for now assume that model uncertainty was not taken into account in the procedure for calibrating the partial factors for soil properties. If this is the case, then using the same limit state function Z_{yield} and the same model variables and type of distribution functions and coefficient of variation, slightly lower partial factors are found for soil properties and the surcharge variable load Q_y.

Since the internal friction angle φ is a dominant design variable, Table 8 shows that the material factors $\gamma_{m;\varphi}$ presently suggested for sheet pile walls in Table A.4b of NEN-EN 9997 (2016) will result in a fairly small differentiation between the reliability classes. Consequently, a design using the partial safety factor associated with RC1 is quite safe, whereas a design per RC3 is presumably too optimistic. Furthermore, the design value found for soil stiffness E_{50} is fairly close to its mean value, and hence a partial factor of 1.3 seems unnecessary.

Table 9. Partial factors γ_m and γ_q for Z_{yield} with correlations between soil conditions for various target reliability indices, for the quay wall without a relieving platform.

Model parameter					Z_{yield}		
Reliability target	X_{rep}, F_{rep}	SI	V		3.3[a]	3.8[b]	4.3[a]
Soil stiffness E_{50}	$X_{k;Low\ 5\%}$	-	0.20	γ_m	0.87	0.90[c,d]	0.92[c]
Tangent of friction angle φ	$X_{k;Low\ 5\%}$	-	0.10	γ_m	1.00	1.03[c,d]	1.07[c]
Weight density γ_{sat}	μ_X	-	0.05	γ_m	1.04	1.04[c,d]	1.05[c]
Surcharge load Q_y	$F_{k;max}$[e]	-	0.10	γ_q	1.11	1.11[d]	1.12
Retaining height $h_{retaining}$	μ_a	cm	n/a	Δ_a	−0.23	−0.26[d]	−0.30
Model factor θ_B	μ_θ	-	0.10	γ_{Rd}	n/a	n/a	n/a
Model factor θ_M	μ_θ	-	0.10	γ_{Sd}	1.12	1.14[d]	1.16

[a]The target reliability index was scaled, while maintaining the sensitivity factors in the U-space.
[b]The obtained reliability indices of 3.76 is very close to this target reliability index.
[c]Partial factor represents the Holocene sand layer for which the internal friction angle is derived at 5% strain rate.
[d]See third column of Table 6.
[e]Operational limit as specified in service level agreement with user.

In the present design codes, correlations between soil properties are not taken into account and no distinction is made between dominant and non-dominant soil layers. Neglecting correlations could lead to an underestimation of the probability of failure, while assuming all soil layers to be dominant may lead to an overestimation. It is therefore recommended that correlations between soil properties be accounted for when defining partial factors, even though this will make the design process more complex.

4.2.3. Example of the derivation of partial factors with model uncertainty

Table 9 presents the partial factors of safety derived from the results of quay wall without the relieving platform, taking into account model uncertainty and correlations. They serve only as an example, since partial factors for codes and standards should ideally be derived from far more reliability-based assessments. Lower partial factors were found for soil stiffness and the surcharge load than recommended in the Eurocode. Furthermore, partial factors for weight density and model factors need to be considered. The partial factors found for the soils' internal friction angle differ widely per reliability class.

5. Conclusion

The results of this study provide guidance on performing finite element-based reliability assessments of real-life quay walls. Its most important findings are as follows.

- Finite element-based reliability assessments have been successfully performed using the gradient-based Abdo-Rackwitz FORM algorithm, which converges quite efficiently and accurately while taking into account a large number of stochastic variables.
- The reliability indices found for critical structural members align with the code requirements. However, they seem quite sensitive to changes in the variation coefficient of variables with a high sensitivity factor, such as the friction angle of soil.
- Neglecting model uncertainty and correlations between input variables leads to an underestimation of the probability of failure.
- The highest sensitivity factors were found for time-independent stochastic variables such as material properties of soil, steel and grout, as well as model uncertainty.
- The local soil stratigraphy and project-specific functional requirements, such as the retaining height and operational loads, can significantly influence the reliability of a quay wall. However, these stochastic variables show low sensitivity factors and hence require relatively low partial factors of safety.
- The differences between the partial factors found for the angle of internal friction of soil in the various reliability classes are greater than the recommended values in the Eurocode standard.

Since it is unclear if and how model uncertainty is accounted for in quay-wall engineering (Gijt and Broeken 2013), it is recommended that the partial factors presently used be re-evaluated and that, for instance, distinctions be drawn between dominant and non-dominant soil layers. In addition, the results of this study show that the variation in the soils' angle of internal friction greatly influences quay-wall reliability. It is therefore recommended that a detailed study be conducted of relevant statistical properties, such as the type of distribution function and its variation coefficient. Furthermore, it is highly recommended that new and existing quay walls be equipped with sensors to reduce the uncertainty related to modelling the soil-structure interaction. Studying this aspect will shed new light on model uncertainty and the actual capacity of a quay wall. The insights obtained will significantly benefit asset managers. Moreover, the data required is quite easy to obtain by simultaneously measuring deformations, water-level differences and anchor forces. This type of information can also be used in Bayesian reliability updating analyses. The finding that time-independent random variables significantly influence the reliability index can play a crucial role in the assessment of existing quay walls, and presumably in that of all other service-proven geotechnical structures. It is therefore highly recommended that further investigation be conducted into the evolution of the probability of failure over time, including the effect of degradation, taking into account the successful service history of the quay walls.

Acknowledgements

On behalf of Delft University of Technology, Deltares, Plaxis, TNO and the Port of Rotterdam Authority, the authors would like to thank all the companies and organisations involved in this study – and SmartPort in particular – for their support, funding and hospitality. Special thanks go to Mr H. Brassinga, who reviewed the finite element models used. Prof. A. C. W. M. Vrouwenvelder, Dr J. G. de Gijt and Mr A. van Seters are gratefully acknowledged for sharing their knowledge and for reviewing the methods used to determine partial factors of safety on behalf of TNO, Delft University of Technology and Fugro respectively. The support and review of Dr R. Lebrun of the OpenTURNS community was of great help during our interpretation of the Abdo-Rackwitz algorithm. Finally, Ms A. Laera and Mr. M. van der Sloot of the Plaxis company are gratefully acknowledged for their

contribution to the development of the ProbAna® reliability interface.

Disclosure statement

No potential conflict of interest was reported by the author(s).

Funding

On behalf of Delft University of Technology, Deltares, Plaxis, TNO and the Port of Rotterdam Authority, the authors would like to thank all the companies and organisations involved in this study – and SmartPort in particular – for their support, funding and hospitality.

ORCID

T. Schweckendiek http://orcid.org/0000-0002-8292-595X

References

Abdo, T., and R. Rackwitz. 1991. *A New Beta-Point Algorithm for Large Time-Invariant and Time-Variant Reliability Problems*. Munich, Germany: Technical University of Munich.

Adel, N. 2018. "Load Testing of a Quay Wall: An Application of Bayesian Updating." MSc thesis. Delft University of Technology, Delft, The Netherlands.

Andrianov, G., S. Burriel, S. Cambier, A. Dutfoy, I. Dutka-Malen, E. de Rocquigny, B. Sudret, et al. 2007. "Open TURNS, An Open Source Initiative to Treat Uncertainties, Risks 'N Statistics in a Structured Industrial Approach." Proceedings of the European Safety and Reliability Conference 2007, ESREL 2007 – Risk, Reliability and Societal Safety 2.

Berg, van der J. W., B. A. S. Seesing, J. Greef, D. J. Jaspers Focks, and P. Quist. 2018. *Quay Wall of the Future: Comparison Report*. Rotterdam: Smartport. RT780-49/18-007.302.

Blum, H. 1931. *Einspannungsverhaltnisse bei Bohlwerken*. Berlin: W. Ernst und Sohn.

Calle, E. O. F., and S. E. J. Spierenburg. 1991. *Veiligheid van Damwandconstructies – Onderzoeksrapportage Deel 1, for CUR Committee C69*. Delft: Deltares. Report CO-31690/12. https://www.deltares.nl/nl/publicaties/.

Cherubini, C. 1999. "Probabilistic Approach to the Design of Anchored Sheet Pile Walls." *Computers and Geotechnics* 26: 309–330.

Cornell, C. A. 1969. "A Probability-Based Structural Code." *ACI Journal* 66: 974–985.

Courage, W. M. G., and H. M. G. M. Steenbergen. 2007. *Prob2BTM: Variables, Expressions and Excel® Installation, and Getting Started*. Delft, The Netherlands: TNO.

Das, M. R., and S. K. Das. 2010. "Reliability Based Optimum Design of Sheet Pile Wall Using a Simple Optimization Tool." Indian Geotechnical Conference, Mumbai, India.

Eijk, R. A. van der. 2011. *Design Report: Quay Wall for a New Bulk Terminal at Maasvlakte Rotterdam*. Rotterdam: Port of Rotterdam Authority.

Gijt, J. G. de, and M. L. Broeken. 2013. *Quay Walls*. 2nd ed. Delft: SBRCURnet.

Hasofer, A. M., and N. C. Lind. 1974. "An Exact and Invariant First Order Reliability Format." *Journal of the Engineering Mechanics Division* 100: 111–121.

Huijzer, G. P. 1996. *Eindrapport Probabilistische Analyse Damwand Constructies*. Rotterdam: Port of Rotterdam Authority.

Huijzer, G. P., and G. Hannink. 1995. "The Construction of Parameterized Subsurface Models." Proceedings, 11th European Conference on Soil Mechanics and Foundation Engineering, Copenhagen, Denmark.

ISO 2394. 2015. *General Principles on Reliability for Structures*. Geneva: International Organisation for Standardisation.

Janssen, H. L. 2012. *CUR 166: Sheet Pile Walls*. 6th ed. Gouda: SBRCURnet.

JCSS. 2001. "Probabilistic Model Code. Part 1. Joint Committee on Structural Safety." www.jcss.byg.dtu.dk.

Jiang, P., A. Basudhar, and S. Missoum. 2011. "Reliability Assessment with Correlated Variables Using Support Vector Machines." 52nd AIAA/ASME/ASCE/AHS/ASC Structures, Structural Dynamics and Materials Conference – Proceedings.

Laera, A., and R. B. J. Brinkgreve. 2017. *Plaxis Probabilistic Analyses 2017. ProbAna*. Delft: Plaxis bv. https://www.povmacrostabiliteit.nl/wpcontent/uploads/2015/03/Prob_Analysis_secured.pdf.

Lemaire, M. 2009. *Structural Reliability*. London: Wiley.

Lindenberg, J. 2008. *Van onzekerheid naar betrouwbaarheid: Handreiking voor geotechnisch ontwerpers*. Gouda: CUR.

Melchers, R. E., and A. J. Beck. 2018. *Structural Reliability Analysis and Prediction*. Hoboken, NJ: Wiley.

NEN-EN 10029. 2010. *Hot-Rolled Steel Plates 3 mm Thick or Above – Tolerances on Dimensions and Shape*. Brussels: European Committee for Standardisation.

NEN-EN 1990. 2011. *Eurocode – Basis of Structural Design*. Brussels: European Committee for Standardisation.

NEN-EN 1997. 2004. *Eurocode 7: Geotechnical Design – Part 1: General Rules*. Brussels: European Committee for Standardisation.

NEN-EN 9997-1. 2016. *National Annex, Eurocode 7: Geotechnical Design – Part 1: General Rules*. Delft: NEN. ICS 91.080.01.

Phoon, K. K., and J. V. Retief. 2016. *Reliability of Geotechnical Structures in ISO239*. Balkema: CRC Press.

Powell, M. J. D. 1994. "A Direct Search Optimization Method That Models the Objective and Constraint Functions by Linear Interpolation." *Advances in Optimization and Numerical Analysis* 275: 51–67.

Rackwitz, R. 2000. "Optimization – the Basis of Code Making and Reliability Verification." *Structural Safety* 22: 27–60.

Rackwitz, R., and B. Fiessler. 1997. "Structural Reliability Under Combined Random Load Sequences." *Computers and Structures* 9: 489–494.

Rippi, A., and A. Texeira. 2016. "Reliability-based Assessment of a Retaining Wall Using FEM." 25th European Young Geotechnical Engineers Conference, Sibiu, Romania.

Roubos, A. A. 2019. *How to use the Abdo-Rackwitz Algorithm in Finite Element-Based Reliability Assessments*. Delft: Delft University of Technology. doi:10.13140/RG.2.2.19421.46568. https://www.researchgate.net/publication/3328

75168_How_to_use_the_Abdo-Rackwitz_FORM_algorithm_in_finite_element-based_reliability_analysis.

Roubos, A. A., D. Allaix, T. Schweckendiek, R. D. J. M. Steenbergen, and S. N. Jonkman. 2020. "Time-dependent Reliability Analysis of Service-Proven Quay Walls Subject to Corrosion-Induced Degradation." *Reliability Engineering & System Safety*.

Schweckendiek, T., A. C. W. M. Vrouwenvelder, E. O. F. Calle, R. B. Jongejan, W. Kanning, et al. 2012. "Partial Factors for Flood Defenses in the Netherlands." In *Modern Geotechnical Codes of Practice – Development and Calibration*, edited by P. Arnold, 311–328. Lansdale: Special Geotechnical Publication, Taylor & Francis.

Teixeira, A., K. Rippi, T. Schweckendiek, H. Brinkman, J. Nuttall, L. Hellebrandt, and W. Courage. 2016. *Soil-Structure Interaction – Reliability Analysis of a Retaining Wall, 2015*. Delft: Deltares & TNO. 11200575-016. https://www.deltares.nl/nl/publicaties/.

Timmermans, A. L. J. 2017. "Final Design, Combi-Wall for Inland Barges, Report Number 101. Project i.000770, Offshore terminal SIF." Rotterdam: Port of Rotterdam Authority.

Well, T.J. van der. 2018. *Reliability-Based Assessment of Quay Walls*. Delft: Delft University of Technology.

Wolters, H. J., K. J. Bakker, and J. G. de Gijt. 2012. *Reliability of Quay Walls Using Finite Element Analysis*. Delft: Delft University of Technology.

Appendices

Appendix 1. Additional information on reference quay walls

Table A1. Settings of finite element models and structural properties of the reference quay walls.

Gerenal	SI	Without relieving platform	With relieving platform
Dimensions	m	100x45	150x51
Higher-order elements	-	4th order 15-nodes	4th order 15-nodes
Construction stage 0	-	Initial stage K0-procedure	Initial stage K0-procedure
Construction stage 1	-	Realisation of construction pit, decrease of water table	Realisation of construction pit, decrease of water table
Construction stage 2	-	Construction of combi-wall	Construction of combi-wall, foundation piles
Construction stage 3	-	Install and prestress anchor system	Realisation of relieving platform and anchor system
Construction stage 4	-	Backfill, dredging works and activation of water levels	Completion of relieving platform, prestress anchors, backfill
Construction stage 5	-	Activate surcharge loads	Dredging works, activation water level differences
Construction stage 6	-	Safety stage[a]	Activate bulk and crane loads
Construction stage 7	-	n.a.	Safety stage[a]
Combi-wall		Plate element	Plate element
Steel quality tube	-	X70	X65
Steel quality sheet pile	-	S355GP	S355GP
E steel	GPa	210	210
EI	kNm^2/m	5.466E+05	1.031 E6
EA	kN/m	3.476E+06	6.058 E6
System length	m	2.995	3.724
Anchor		Grout anchor	Grout anchor
Strut	-	Note to node	Node to node
Grout	-	Embedded beam row	Embedded beam row
Steel quality	-	E470	AC600D
Strut diameter	mm	101.6	82.5
Wall thickness strut	mm	17.5	22.2
Centre to centre	m	1.47	2.735
Level	-	NAP+1.50m	NAP+0.9m
EA	kN per pile	9.7E5	n/a
..	kN/m	n/a	310.5 E3
E grout body	kN/m^2 per pile	7E6	n/a
..	$kN/m^2/m$	n/a	2.10 E8
τ_{skin}	kN/m	750	330
Inclination	°	45	18
Foundation piles		n/a	Embedded beam row
Inclination	-	n/a	1:3.5
Diameter	m	n/a	0.560/0.650
Centre to centre	m	n/a	2.28
EI	kNm^2/m	n/a	21.17 E3
EA	kN/m	n/a	1.08 E6
τ_{skin}	kN/m	n/a	100

[a]In case of geotechnical limit states and additional safety stage was added.

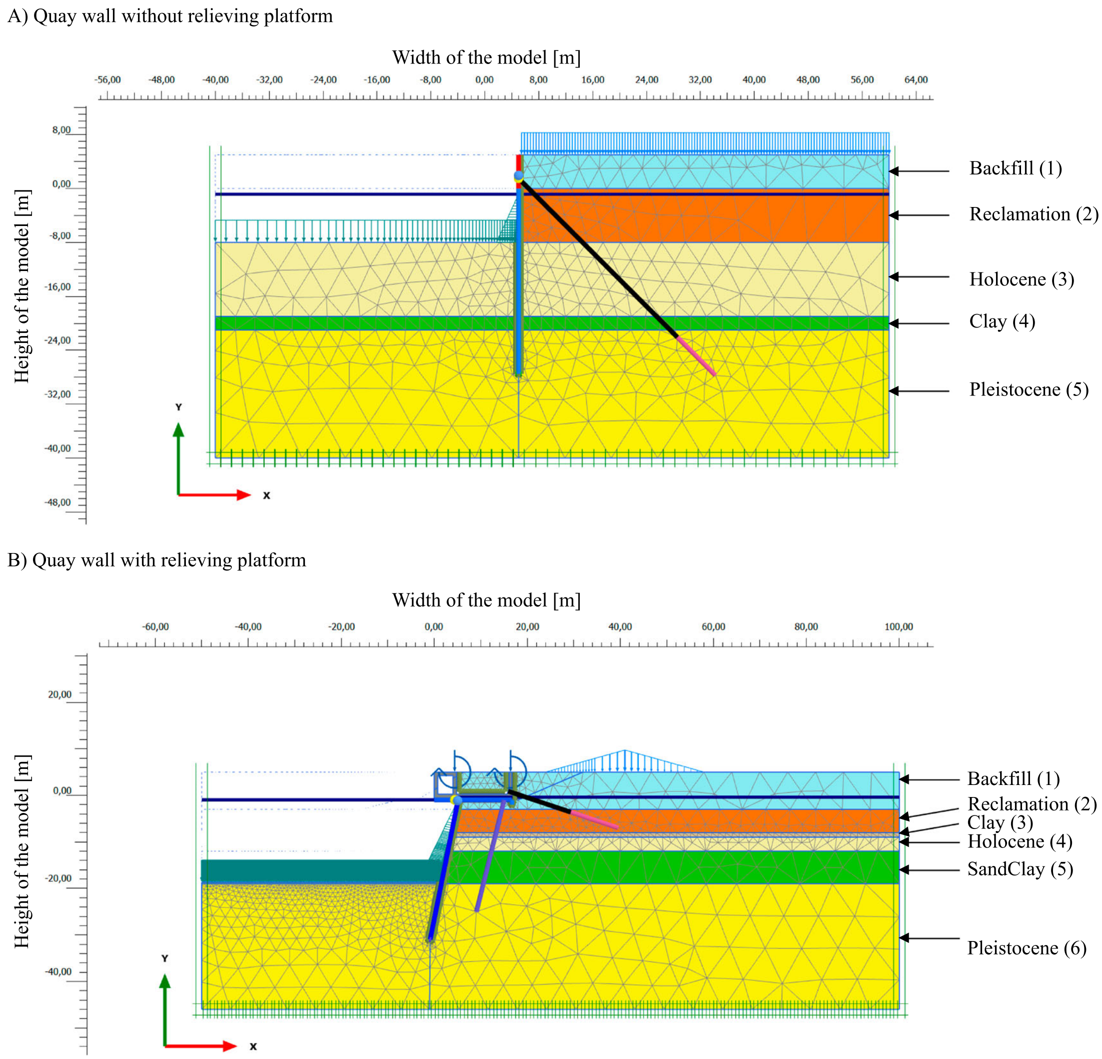

Figure A1. Finite element model of the reference quay walls: (A) Quay wall without the relieving platform and (B) Quay wall with relieving platform.

Appendix 2. Model variables and distribution functions

Table A2. Stochastic model variables and the associated marginals of their distribution function for the reference quay wall, without and with a relieving platform.

Random variables	SI	Characteristic value	Without relieving platform		With relieving platform		Type of distribution function	CoV or Δa
Materials X_i	-	$X_{i;k}$	μ_x	$X_{i;k}$	μ_x	$X_{i;k}$	-	V_x
$E_{50;Backfill}$	MPa	μ_X [a]	50	50	35	35	Lognormal	0.2
$E_{50;Reclamation}$	..	..	30	30	75	75	..	..
$E_{50;Clay}$	..	..	5	5	8	8	..	..
$E_{50;Holocene}$	..	..	30	30	22	22	..	..
$E_{50;SandClay}$	..	..	n/a	n/a	10	10	..	..
$E_{50;Pleistocene}$	..	..	50	50	60	60	..	..
$\varphi_{;Backfill}$ [b]	°	$X_{i;5\%}$	38.9	32.5	38.9	32.5	Normal	0.10
$\varphi_{;Reclamation}$ [b]	..	..	35.9	30	41.8	35	..	..
$\varphi_{;Clay}$ [b]	..	..	26.9	22.5	26.9	22.5	..	..
$\varphi_{;Holocene}$ [b]	..	..	35.9	30	38.9	32.5	..	..
$\varphi_{;SandClay}$ [b]	..	..	n/a	n/a	32.3	27	..	..
$\varphi_{;Pleistocene}$ [b]	..	..	38.9	32.5	41.8	35	..	..
$\gamma_{sat;\ Backfill}$	kN/m^3	μ_X	20	20	18	18	Normal	0.05

(*Continued*)

Table A2. Continued.

Random variables Materials X_i	SI -	Characteristic value $X_{i;k}$	Without relieving platform μ_x	$X_{i;k}$	With relieving platform μ_x	$X_{i;k}$	Type of distribution function -	CoV or Δa V_x
$\gamma_{sat;Reclamation}$	..	..	20	20	20	20	..	..
$\gamma_{sat;Clay}$	..	..	17	17	17.1	17.1	..	..
$\gamma_{sat;Holocene}$	..	..	20	20	20	20	..	..
$\gamma_{sat;SandClay}$	..	..	n/a	n/a	19	19	..	..
$\gamma_{sat;Pleistocene}$	..	..	20	20	21	21	..	..
c_{Clay}	kPa	$X_{i;5\%}$	6.9	5	13.9	10	Lognormal	0.20
$c_{SandClay}$	..	..	n/a	n/a	13.9	10	..	..
$f^c_{y;tube}$	N/mm^2	$X_{i;5\%}$	517	485	483	455	..	0.04[c]
$f^c_{y;anchor}$	..	..	539	515	641	600	..	..
α_t	-	$X_{i;5\%}$	0.018	0.015	0.018	0.015	Normal[d]	0.10[d]
q_c	MPa	μ_X	15	15[e]	10	10[e]	..	0.10[f]
Loads F_i	-	$F_{i;k}$	μ_F	$F_{i;k}$	μ_F	$F_{i;k}$	-	V_F
$Q_{surcharge}$[g]	kN/m^2	Nominal[h]	104.8	100	41.9	40	Gumbel	0.10[g]
Q_{bulk}[g]	..	..	n/a	n/a	178.2	170	..	..
F_{crane}[g]	kN	$F_{i;TR=50}$	n/a	n/a	628.7	600	..	..
$F_{bollard}$[g]	..	SWL[i]	35.9	34.3	104.8	100	..	..
Geometry a_i	-	$a_{i;k}$	μ_a	$a_{i;k}$	μ_a	$a_{i;k}$	-	Δa
h_{OWL}	m	LLWS[i]	−0.96	−0.84	−0.96	−0.84	Gumbel	0.20m
h_{GWL}	..	$h_{drainiage}$+0.3m	−0.40	−0.34	−0.40	−0.34	..	0.25m
$h_{retaining}$	m to MSL[i]	μ_a	−27.5	−27.5	−31.5	−31.5	..	0.35m[j]
h^c_{pile}	m	..	−8	−8	−18.5	−18.5	..	0.35m[c]
$D_{SoilLayer}$	..	..	varies	varies	varies	varies	..	..
D^c_{tube}	..	..	1.067	1.067	1.420	1.420	Normal	V_a=0.05[c]
t^c_{tube}	..	..	0.015	0.015	0.016	0.016	..	..
L^c_{grout}	..	..	8.5	8.5	12	12	..	V_a=0.04[c]
O^c_{grout}	..	..	1.31	1.31	1.06	1.06	..	..
Model uncertainty θ_i	-	$\theta_{i;k}$	μ_θ	$\theta_{i;k}$	μ_θ	$\theta_{i;k}$	-	V_θ
θ_M	..	..	1	n/a	1	n/a	Lognormal	0.10
θ_N; θ_F	..	..	1	n/a	1	n/a	..	0.10
θ_{Msf}	..	..	1	n/a	1	n/a	..	0.10

[a]Mean values were derived on the basis of empirical correlations with the cone resistance.
[b]Analogous with Table 2.1b, NEN-EN 9997 (2016), considered at 5% strain rate.
[c]Based on production and execution tolerances as well as project-specific acceptance criteria in the port of Rotterdam.
[d]Little information is available in the literature. In this study, a normal distribution was assumed. The values are based on full-scale field tests (Well 2018).
[e]Based on maximum allowable cone resistance (cut-off), in accordance with design guidance (Janssen 2012).
[f]Based on soil investigation used in the design of the quay wall.
[g]Extreme value distribution for a reference period of 50 years.
[h]The characteristic value is based on an operational limit.
[i]LWWS = low low water at spring tide; SWL = safe working load; MSL = mean sea level.
[j]Based on expert judgement. This also considers small morphological changes, erosion and sedimentation. The effect of large scour holes and deepening the harbour bottom were not taken into consideration.

Appendix 3. Comparison of Blum & Prob2B with Plaxis & OpenTURNS

Table A3. Comparison of Blum & Prob2B with Plaxis & OpenTURNS in respect of lifetime reliability index, the design points in physical space X^* and normal space U^* and the sensitivity factor α for Z_{yield}.

		Blum & Prob2B			Plaxis & OpenTURNS		
Reliability index β		3.87			3.76		
Parameter	SI	X^*	U^*	$\alpha_{u\text{-}space}$	X^*	U^*	$\alpha_{u\text{-}space}$
$E_{50;Backfill}$	MPa	n/a	n/a	n/a	50.9	0.19	0.05
$E_{50;\ Reclamation}$	MPa	n/a	n/a	n/a	25.7	−0.68	−0.19
$E_{50;\ Holocene}$	MPa	n/a	n/a	n/a	24.3	−0.96	−0.26
$E_{50;\ Clay}$	MPa	n/a	n/a	n/a	4.8	−0.07	−0.02
$E_{50;Pleistocene}$	MPa	n/a	n/a	n/a	49.2	0.02	0.01
$\varphi_{\ Backfill}$	°	39.4	0.13	0.03	39.7	0.16	0.04
$\varphi_{\ Reclamation}$	°	33.1	−0.78	−0.20	30.6	−1.34	−0.37
$\varphi_{\ Holocene}$	°	24.7	−3.11	−0.80	29.4	−1.60	−0.44
$\varphi_{\ Clay}$	°	26.6	−0.12	−0.03	26.7	−0.07	−0.02
$\varphi_{\ Pleistocene}$	°	38.6	−0.06	−0.02	39.3	0.09	0.03
$\gamma_{sat;\ Backfill}$	kN/m^3	20.3	0.32	0.08	20.5	0.41	0.11
$\gamma_{sat;\ Reclamation}$	kN/m^3	20.0	0.45	0.12	19.3	0.17	0.05
$\gamma_{sat;\ Holocene}$	kN/m^3	17.8	−0.77	−0.20	18.6	−0.39	−0.11
$\gamma_{sat;\ Clay}$	kN/m^3	17.0	0.00	0.00	16.9	−0.06	−0.02
$\gamma_{sat;\ Pleistocene}$	kN/m^3	20.0	0.01	0.00	20.1	0.03	0.01

(Continued)

Table A3. Continued.

		Blum & Prob2B			Plaxis & OpenTURNS		
Reliability index β		3.87			3.76		
Parameter	*SI*	X^*	U^*	$\alpha_{u\text{-}space}$	X^*	U^*	$\alpha_{u\text{-}space}$
h_{OWL}	m	−0.82	0.06	0.01	−0.84	0.01	0.00
h_{GWL}	m	−0.27	−0.24	−0.06	−0.31	−0.22	−0.06
Q_{t50}	kN/m^2	116	1.12	0.29	112	0.61	0.17
$h_{retaining}$	m	n/a	n/a	n/a	0.25	−0.72	−0.20
t_{tube}	mm	14.6	−0.53	−0.14	14.5	−0.67	−0.18
D_{tube}	m	1.029	−0.72	−0.19	1.021	−0.86	−0.24
f_y	N/mm^2	479.7	−0.84	−0.22	473.8	−1.74	−0.48
θ_M	-	1.10	0.96	0.25	1.14	1.36	0.37
θ_N	-	1.02	0.24	0.06	1.04	0.36	0.10